Contents lists available at ScienceDirect

Food and Bioproducts Processing

journal homepage: www.elsevier.com/locate/fbp

Corn starch systems as carriers for yerba mate (*Ilex paraguariensis*) antioxidants: Effect of mineral addition

A.S. Teixeira[a], A.S. Navarro[a,c], A.D. Molina-García[b], M. Martino[a], L. Deladino[a,*]

[a] Centro de Investigación y Desarrollo en Criotecnología de los Alimentos (CIDCA), CONICET, Fac. Cs. Exactas (UNLP), 47 y 116, La Plata 1900, Argentina
[b] Instituto Ciencia y Tecnología de Alimentos y Nutrición (ICTAN-CSIC), José Antonio Novais 10, 28040 Madrid, Spain
[c] Fac Ingeniería (UNLP), 1 y 47, La Plata 1900, Argentina

ARTICLE INFO

Article history:
Received 21 July 2014
Received in revised form 5 January 2015
Accepted 12 January 2015
Available online 17 January 2015

Keywords:
Starch
High hydrostatic pressure
Minerals
Natural antioxidants

ABSTRACT

Corn starch is considered a good vehicle for delivering bioactive compounds such as supplements or health promoting additives. The ability of starch treated by high hydrostatic pressure (HHP) to bind and carry zinc and magnesium salts and natural antioxidants of yerba mate (*Ilex paraguariensis*) extracts was tested. A uniform distribution of the minerals on the surface of starch granules was observed by SEM–EDX and significantly higher amounts of minerals were loaded by HHP treated starches. Calorimetric analysis showed the effect of both HHP treatment and the active compounds addition, while crystal fraction was determined by X-ray diffraction, denoting the presence of minerals in the starch granule. It was found that the type of starch carrier did not affect total polyphenol loading. Besides, HPLC analysis showed that the relative composition of polyphenols from yerba mate extract was maintained. These results support the use of HHP treated corn starch as an alternative carrier for molecules of nutritional interest into food systems.

1. Introduction

Starch is the major carbohydrate reserve in higher plants. In contrast with cellulose that is present in dietary fiber, starch is digested by humans and represents one of the main sources of energy to sustain life. Bread, potato, rice and pasta are examples of the importance of starch in our society (Carvalho, 2013). In 2000, the world starch market was estimated to be 48.5 million tons, including native and modified starches. The value of the output is worth €15 billion per year, explaining the industrialists and researchers seeking new properties or high value applications (Le Corre et al., 2010; Rodrigues and Emeje, 2012).

Starch gelatinization is an important physical phenomenon in food processing and has been described extensively over the last 40 years (Anderson et al., 1969; Aparicio et al., 2009; Chiang and Johnson, 1977; Fu et al., 2014; Simonin et al., 2011; Wootton et al., 1971). Besides, the microstructure of starch significantly affects its processing characteristics. During chemical reactions, reagents cannot penetrate easily into the granule's interior. As a consequence, reactions often take place only on the surface of the granule and the process efficiency of native starch is usually low.

Gelatinization of starch can be achieved not only by temperature control and water but also by high hydrostatic pressure treatment. The pressure required for full gelatinization depends on the starch type. Gelatinization was achieved at 450 MPa for wheat starch, 550 MPa for maize starch, and 800 MPa for potato starch in 25% suspensions (Stute et al.,

* Corresponding author.
E-mail address: loredeladino@gmail.com (L. Deladino).
http://dx.doi.org/10.1016/j.fbp.2015.01.002

1996). For wheat starch, zero crystallinity as measured by DSC was attained at 600 MPa (Douzals et al., 1996). When lower pressure levels are applied (300–400 MPa), a partially gelatinized product is obtained, which retains some of the granular characteristics which are lost in fully gelatinized systems. These granules show an open network of amylose and amylopectin protruding chains which are prone to interact with a number of potentially useful ligands (Fernández et al., 2008).

Ilex paraguariensis St. Hilaire (Aquifoliaceae) is a native tree from Northeastern Argentina, but it is also cultivated in Southern Brazil and Eastern Paraguay. It is one of the best known and used species in South America, since the product obtained from its industrialization, yerba mate, is used to prepare tea-like beverages (infusions or decoctions). This beverage is appreciated for its peculiar flavor and stimulating and nutritional properties; it also presents antioxidant activity, ascribed to its chemical compounds, such as caffeic and chlorogenic acids and their derivatives (Bracesco et al., 2011; Filip et al., 2007; Gorzalczany et al., 2001). Moreover, the leaves have a considerable amount of minerals and other inorganic compounds such as calcium, sodium, chlorine, potassium, copper, chromium, aluminum, manganese, magnesium, nickel, iron and zinc which must be included in the human diet (Heck and González de Mejía, 2007). However, not all of these compounds are entirely dissolved during water extraction, since some phenolic compounds and minerals are retained and discarded with wasted mate leaves (Bracesco et al., 2011).

Humans require at least 22 mineral elements for their wellbeing (Graham et al., 2001; White and Broadley, 2005). Healthy people can have these supplied by an appropriate diet. However, it is estimated that over 30% of the world's 6 billion habitants are zinc deficient. In addition, magnesium deficiency is common in many developed and developing countries (Grusak and Cakmak, 2005; Rude and Gruber, 2004; Thacher et al., 2006). This situation is attributed to crop production in areas with low mineral phytoavailability and/or consumption of (staple) crops with inherently low mineral tissue concentrations, combined with a lack of fish or animal products in the diet (Graham et al., 2001; Poletti et al., 2004; White and Broadley, 2005). Currently, mineral malnutrition is considered to be among the most serious global challenges to humankind but it is avoidable (Meenakshi, 2009). Mineral malnutrition can be addressed through dietary diversification, mineral supplementation, food fortification and/or increasing mineral concentrations in edible crops (biofortification). Food biofortification combined with availability, is encouraged as an immediate strategy to spread mineral consumption (Bouis et al., 2003; Genc et al., 2005; Graham et al., 2001; Pfeiffer and McClafferty, 2007; White and Broadley, 2005).

The effect of zinc and magnesium absorption in the presence of polyphenols has been poorly explored; more attention has been focused on iron absorption. Hamdaoui et al. (1997) found that tea decoction significantly increased zinc, copper and magnesium concentrations in the total blood of healthy rats. Also, Etcheverry et al. (2012) found that polyphenols did not interfere with the zinc absorption while studying the *in vitro* bioaccessibility and bioavailability methods for different bioactive compounds.

In a previous work (Deladino et al., 2014), native and high pressure treated corn starches were used as suitable carriers for natural antioxidants of yerba mate extracts. The present work is focused on the ability of these starches to also bind zinc and magnesium salts, either alone or mixed with yerba mate extracts. Such studies are of particular importance because polyphenols and minerals have shown to differ considerably on their bioactivity. Thus, these findings may contribute to the selection of suitable material combinations for new functional foods.

2. Experimental

2.1. Preparation of starch carriers

Carrier systems were either native corn starch (S) (Molinos Río de La Plata, Argentina) or high pressure treated starch (HPS) as described in previous studies (Deladino et al., 2014). High pressure starches were obtained by suspending 10 g/100 mL of the aforesaid starch in deionized water (Milli-Q, Millipore Inc. Bedford, MA, USA). A HHP Pilot Food Processor (Stansted Fluid Power LTD. Model FP 571000:9/2C, UK) was operated under 400 MPa, for 35 min with an initial vessel temperature of 38 °C and reaching a final process temperature of 40 °C. Starches were dried in an oven at 30 °C, powdered in a mortar and stored at room temperature in hermetic boxes.

2.2. Characterization of starch carriers

2.2.1. Optical microscopy

Observations of starch suspensions were carried out with an Olympus BX41 microscope (Olympus, Tokyo, Japan), using transmitted light, equipped with an Olympus DP70 microscope camera (Olympus, Tokyo, Japan).

2.2.2. Porosimetry

Pore size and pore volume were measured with a mercury porosimeter (AutoPore IV 9500, USA). Samples were dried at 80 °C for 24 h and degassed for 5 min at 484 dynes/cm before analysis. Assays were carried out under controlled temperature conditions at 22 °C (±2 °C).

Pore sizes were calculated using the Washburn equation:

$$D = -\left(\frac{1}{P}\right) 4\gamma \cos\varphi \quad (1)$$

where D (nm) is the pore diameter and P (MPa) the applied pressure for mercury intrusion, assuming that pores were cylindrical in shape, the solid–liquid contact angle (φ) was 141° and the surface tension (γ) of mercury was 484 dyn/cm (Fornal et al., 2012). The highest intrusion pressure reached was 200 MPa.

Intraparticle volume was calculated as the volume of mercury intruded after the last inflection point of the intrusion/extrusion curve (Beirão-da-Costa et al., 2011).

2.3. Preparation of active starches with minerals and yerba mate extract

A lyophilized yerba mate extract (Y) was obtained as described elsewhere (Deladino et al., 2008). Briefly, the extracts were obtained as follows: 1 g of commercial yerba mate (Las Marías, Corrientes, Argentina) was mixed with 100 mL of distilled water in a glass vessel, heated in a thermostatic bath (Haake, Germany) at 100 °C for 40 min. Then the extract was filtered, frozen at −80 °C for 24 h and lyophilized in a Heto FD4 equipment (Denmark). The yield of the process was 32.7% dry basis. Lyophilized extracts were stored in a dissecator in tightly closed flasks.

Table 1 – Nomenclature of samples prepared by different treatments.

	Active compound						
Starch	Y	Zn	Mg	Zn + Mg	Zn + Y	Mg + Y	Zn + Mg + Y
S	S_Y	S_{Zn}	S_{Mg}	S_{ZnMg}	S_{ZnY}	S_{MgY}	S_{ZnMgY}
HPS	HPS_Y	HPS_{Zn}	HPS_{Mg}	HPS_{ZnMg}	HPS_{ZnY}	HPS_{MgY}	HPS_{ZnMgY}
HPS*	HPS^*_Y	HPS^*_{Zn}	HPS^*_{Mg}	HPS^*_{ZnMg}	HPS^*_{ZnY}	HPS^*_{MgY}	HPS^*_{ZnMgY}

S = commercial starch, HPS = HHP treated starch, HPS* = *in situ* HHP treated starch, Y = yerba mate extract.

The mineral salts solutions were prepared at 0.05 M with $MgSO_4 \cdot 7H_2O$ and $ZnSO_4 \cdot H_2O$ (Panreac, Spain). The lyophilized yerba mate extract was dissolved in water (0.1 g/100 mL). Starch aqueous suspensions were prepared mixing 10 g of starch in 100 mL of the above described solutions. Several types of products were obtained (Table 1):

HPS_{Mg}, HPS_{Zn} and HPS_{ZnMg} or S_{Mg}, S_{Zn} and S_{ZnMg}: suspensions of HPS and S carriers were prepared in salts solutions, placed in dark glass bottles and agitated in an orbital shaker (Orbit Environ Shaker, Lab Instruments, USA) at 25 °C and 180 rpm for 15 h (Immersion procedure, Fig. 1A). Similar samples were obtained with yerba mate extract (HPS_{MgY}, HPS_{ZnY} or HPS_{ZnMgY} and S_{MgY}, S_{ZnY} or S_{ZnMgY}). In the case of samples with two salts, 0.05 M of each one was employed.

HPS^*_{Mg}, HPS^*_{Zn} and HPS^*_{ZnMg}: the commercial starch (S) was suspended in the salts solutions and then the resultant mixture was submitted to high pressure treatment (*in situ* procedure, Fig. 1B), as described in Section 2.1. All samples obtained under *in situ* procedure will be denoted by an asterisk following HPS (HPS*). Similar samples were obtained with yerba mate extract (HPS^*_{MgY}, HPS^*_{ZnY} or HPS^*_{ZnMgY}). In the case of samples with two salts, 0.05 M of each one was employed.

All suspensions were centrifuged (Rolco, USA, 20 min, 300 × *g*) and the supernatant was discarded. Samples were dried in an oven at 30 °C. The obtained products were powdered in a mortar and stored in hermetic boxes. Also mixtures of both minerals and minerals with yerba mate extract were obtained, so a detail of the applied treatments and the nomenclature of samples are shown in Table 1. Unless otherwise indicated, all assays were performed in triplicate.

2.4. Characterization of active starches

2.4.1. Scanning electron microscopy (SEM–EDX)

Mineral distribution on the granule surface was observed by SEM, using a ZEISS DSM-960 microscope, equipped with an EDX (ISIS-LINK, Oxford Instruments, UK) system. Directly before analysis, powdered samples were sprinkled on conductive bands and coated with a thin layer of carbon.

2.4.2. X-ray diffraction

Starch samples were analyzed in an X-ray diffractometer X'Pert Pro PANalytical Model PW3040/60 (Almelo, Netherland) using a Cu Kα radiation (λ = 1.54186 Å), at 40 kV and 40 mA. Diffractograms were obtained between 2θ = 3–60°.

X-ray diffraction (XRD) patterns of starch aggregates are characterized by sharp peaks associated with the crystalline diffraction and an amorphous zone. The amorphous fraction of the sample can be estimated by the area between the smooth curve drawn following the scattering hump, and the baseline joining the background within the low and high-angle points. The crystalline fraction (CF) was calculated as the ratio between the absorption peaks and the total diffractogram area, expressed as percentage (%) (López and García, 2012; Mali et al., 2006). Also, the crystalline fraction attributed to mineral incorporation was estimated from X-ray data as follows:

$$\text{mineral crystalline fraction} = (CF_{\text{active starch}} - CF_{\text{control starch}}) \times 100 \quad (2)$$

where the control starch was the corresponding starch carrier depending on the sample (S, HPS or HPS*). The reported values corresponded to the average of two determinations.

2.4.3. Differential scanning calorimetry (DSC)

Differential scanning calorimetry determinations were performed with a DSC Q100 (TA Instruments, USA), calibrated with an Indium standard, at a scanning rate of 10 °C/min, heating from 25 to 110 °C. To minimize hydration variability, starch samples were dispersed in water (20% w/w) 24 h before DSC analysis. Then, 15 μL of slurry were introduced in weighted aluminum pans, sealed and re-weighed. After analysis, pans were punctured and dried at 110 °C to constant weight, to ensure accurate moisture and starch content determinations. Thermograms were analyzed following standard procedures (Universal Analysis Program, TA Instruments); Onset (T_o) and peak temperature (T_p) and gelatinization enthalpies (ΔH) were calculated. Analyzes were performed at least in triplicate.

2.5. Determination of active compounds in starches

2.5.1. Mineral salts

An atomic emission spectrometer (ICP–OES) Optima 3300 DV Perkin Elmer (USA) was employed. Before determination, samples were digested to transform them from solid to liquid. Acid digestion ($HNO_3 + HCl + HF + H_3PO_4$) was carried out in a closed vessel in a high pressure digesting microwave (MW-AP Multiwave 3000, Anton Paar, UK). Liquid sample was streamed and atomized by argon plasma. The atomic stream emits a characteristic radiation depending on the element and its concentration is proportional to the intensity of the emitted signal. An external calibration method was employed.

2.5.2. Total polyphenols

A known amount of starch was suspended in water and agitated for 24 h in the orbital shaker, then samples were centrifuged and total polyphenols content was determined by the Folin–Ciocalteau method as described in a previous work (Deladino et al., 2008).

High performance liquid chromatography (HPLC) and mass spectrometry (MS) were used to identify the components of bioactive starches, based on their retention times and MS spectra, and by comparing with pure standards and

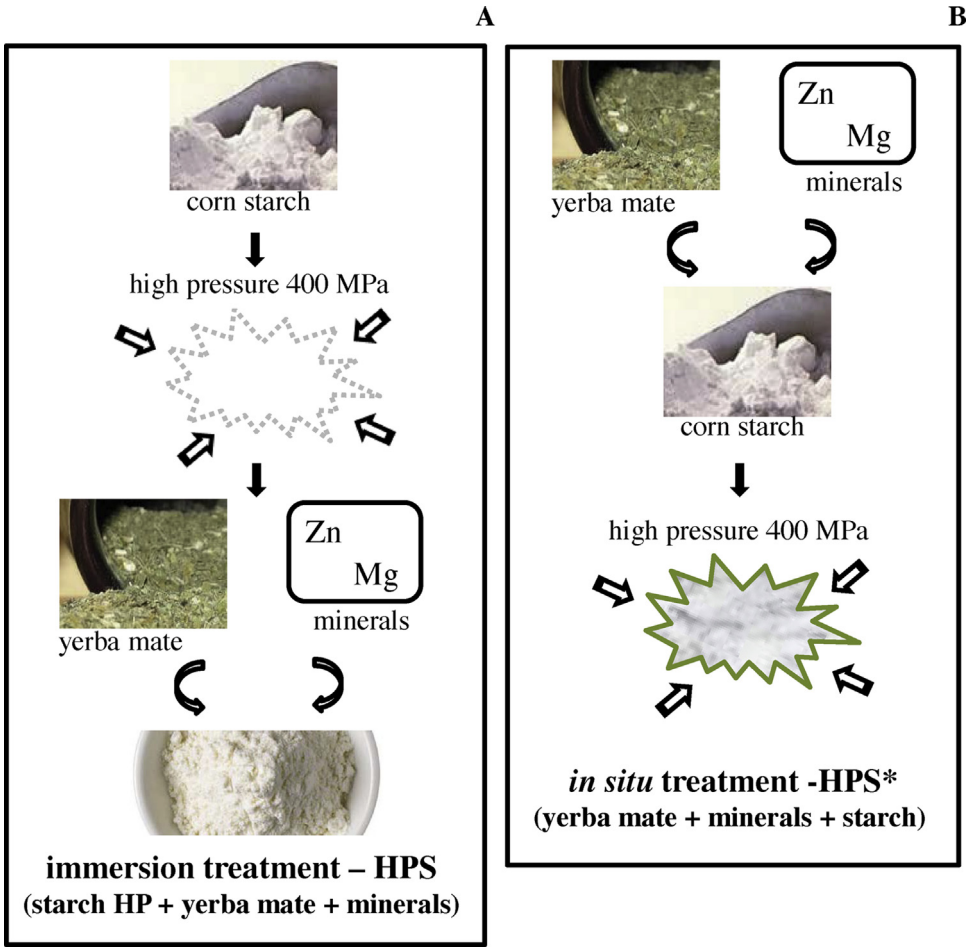

Fig. 1 – Scheme of the steps of the protocol employed, see text for more information. Immersion treatment (A) and *in situ* treatment (B).

literature data. Samples were subjected to several extractions with Milli Q water (1 mL). Aliquots were collected and mixed before determining polyphenol content. A lyophilized yerba mate extract was also analyzed as a control.

Analyses were performed using Agilent 1100 series LC equipment, comprised of a quaternary pump with integrated degasser, autosampler, thermostated column compartment and diode array detector (DAD), coupled with an Agilent G1946D Quadrupole mass spectrometer (Agilent Technologies, Waldbroon, Germany). Data acquisition and analysis were carried out with an Agilent ChemStation Software. Samples of 20 μL were separated in a 150 mm × 4.6 mm i.d., 5 μm, C18 Agilent Zorbax Eclipse XDB-C18 analytical column (Agilent), eluted with a mobile phase of a mixture of deionized water (solvent A) and acetonitrile (solvent B), both containing 0.1% formic acid, at a flow rate of 1 mL/min. The solvent gradient changed according to the following conditions: from 90% A to 74% A in 40 min, to 35% A in 10 additional min, and then returning to the initial conditions after 5 min more. Because of the lack of commercial standards, chlorogenic acid esters and isomers were quantified as chlorogenic acid.

Mass spectrometry data were acquired in the scan mode (mass range *m/z* 100–1100). Ions were produced by atmospheric pressure electrospray ionization (ESI). This source was operated in the negative ion mode, with the electrospray capillary voltage set to 3500 V, a nebulizing gas flow rate of 12 L/h, and a drying temperature of 350 °C. For negative polarity, *m/z* 179 (rutin), 353 (chlorogenic acid and isomers) and 515 (chlorogenic acid esters) were used as standards. These compounds were quantified from the areas of their chromatographic peaks by comparison with calibration curves. Chlorogenic acid and rutin standards were specific for HPLC assay, and their purity was ≥95% (Sigma, St. Louis, MO, USA).

2.6. *Statistical analysis*

Analysis of variance (ANOVA) and mean comparisons were performed with the software SYSTAT INC. (Evanston, USA). were carried out. Unless indicated, a level of 95% confidence ($\alpha = 0.05$) was used.

3. Results

3.1. *Characterization of starch carriers*

Fig. 2 shows the effect of high hydrostatic pressure on corn starch. As expected, native starch granules showed the smallest granule sizes and almost all exhibited the typical Maltese crosses under polarized light (Fig. 2A and B). This fact evidenced the partially crystalline structure of corn starch granules. High pressure treatment partially gelatinized the starch granules, as seen by increased granule sizes due to a limited swelling (Fig. 2C). In Fig. 2D some granules maintained the same Maltese crosses as the native starch after HHP treatment.

Porosimetry analysis helped understand the effect of the different treatments. Fig. 3 shows the pore diameter distribution for native and HHP treated starches. Non-treated corn

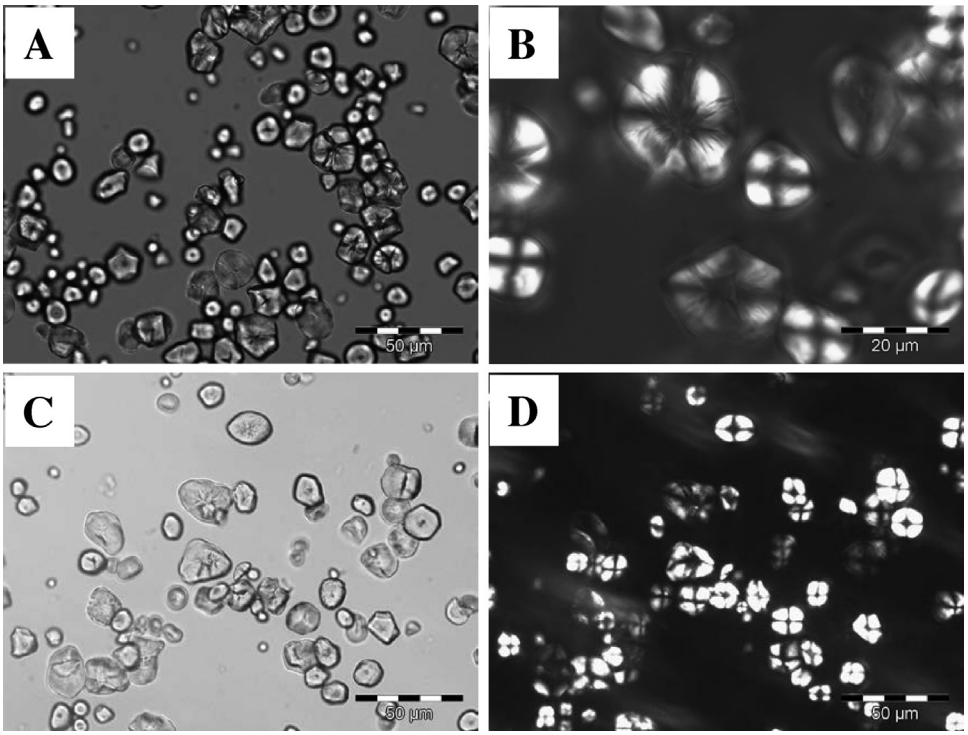

Fig. 2 – Optical micrograph of native and high hydrostatic pressure corn starch (A and B) native corn starch (S); (C and D) high pressure treated starch (HPS), (B and D) micrographs were taken under polarized light.

starch showed a broad distribution of pore diameters ranging from 8 to 60 nm (micropores), with a maximum number of pores between 8 and 12 nm. The high pressure treatment caused a narrowing in this profile, with pore diameters ranging from 2 to 12 nm, and increased the total volume (total surface area) of pore with a maximum number of pores between 4 and 10 nm. This fact was attributed to granule reorganization during partial gelatinization due to high pressure. Taking into account the total pore volume (mL of mercury/g starch), the porosity of starch carriers was higher in HPS samples compared to the native starches (Fig. 3). These results confirmed the observations found when surface area and pore size distribution of starch carriers were analyzed by different techniques (nitrogen adsorption/desorption isotherms and confocal laser scanning microscopy) (Deladino et al., 2014). An increased exposed surface area suggests higher potential binding sites (Fernández et al., 2008), which could be occupied by active compounds like minerals and antioxidants.

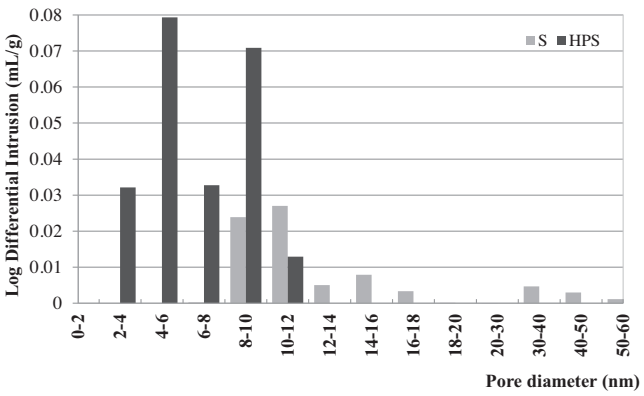

Fig. 3 – Pore size distribution of starch carriers determined by mercury porosimetry. Native corn starch (S); high pressure treated starch (HPS).

3.2. *Characterization of bioactive starches*

3.2.1. *Scanning electron microscopy (SEM–EDX)*

Starch microstructure can be examined using SEM as this technique allows high-resolution imaging of granules. All starches granules loaded with minerals showed the presence of the corresponding salt on their surface (Fig. 4). However, the HHP treatment clearly influenced the amount of mineral adsorbed on the surface, whereas in contrast, non-treated starch showed few mineral dots. Accordingly, other authors also reporting changes in the surface characteristics of pressurized granules by SEM, which indicated significant alterations in the internal structure (Stolt et al., 1999; Stute et al., 1996; Tao et al., 2012). In samples HHP-treated by immersion, a preferential adsorption of zinc was observed (Fig. 4 HPS_{Zn}). The higher amounts of minerals were detected after *in situ* HHP treatment (Fig. 4 HPS*Zn and HPS*Mg).

3.2.2. *Crystalline fraction by X-ray diffraction*

X-ray diffractometry has been used to study starch crystallinity (Mali et al., 2006) in order to obtain a quantitative estimation of the extent of gelatinization. The crystallinity of starch is known to decrease with gelatinization; a completely gelatinized starch has an amorphous structure.

The XRD patterns observed from S and HHP carriers and some bioactive systems are shown in Fig. 5. Native corn starch showed a typical A-type XRD pattern with characteristic peaks at 2θ: 5.18, 5.79, 15.3, 17.1, 18.2, and 23.5. In HHP carrier, the pattern was the same but with a clear shift to lower 2θ values in the first half of the diffractogram (Fig. 5A). Katopo et al. (2002) while studying starches pressurized under the presence of water, found that starches of the A-type X-ray pattern went through a transformation from the A-type pattern to the B-type pattern. In the present work, no peaks of B-type diffraction pattern were observed in treated samples. Fig. 5B shows bioactive starches obtained under high

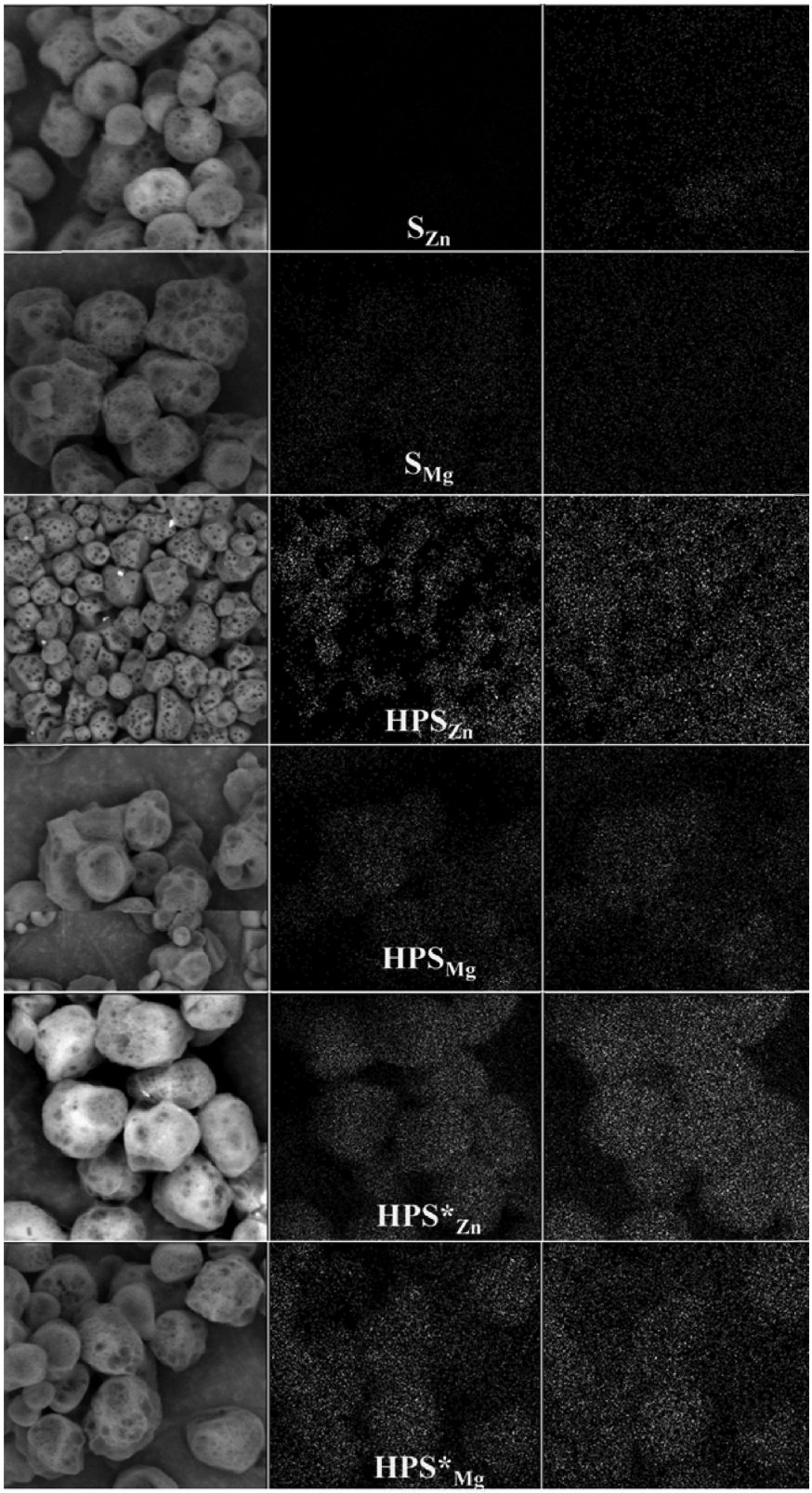

Fig. 4 – SEM–EDX micrographs. Left column shows the SEM photograph, center column shows Zn or Mg mapping and right column shows sulphur mapping in each sample. 2000× with except of HPS_{Zn} (500×). Nomenclature is referred in Table 1.

pressure *in situ* procedure with main peaks at 21.07° for magnesium sulphate heptahydrate and at 20.26° for zinc sulphate hexahydrate (JCPDS-International Centre for Diffraction Data; Paulik et al., 1981; Spiess and Gruehn, 1979; Walenta, 1978). In samples containing zinc and magnesium together, a contribution of peaks from both salts was observed, also peaks corresponding to tetrahydrated zinc salt and $MgZn(SO)_4{\cdot}H_2O$ were observed. Hydration from dissolution and recrystallization of salt with different water content on the starch granule surface would have taken place. The original salt ($ZnSO_4{\cdot}H_2O$) crystallizes according the medium conditions (pressure, temperature, concentration, time). The characteristic peaks of each salt could not be detected in the bioactive starches obtained under HHP immersion procedure (data not shown).

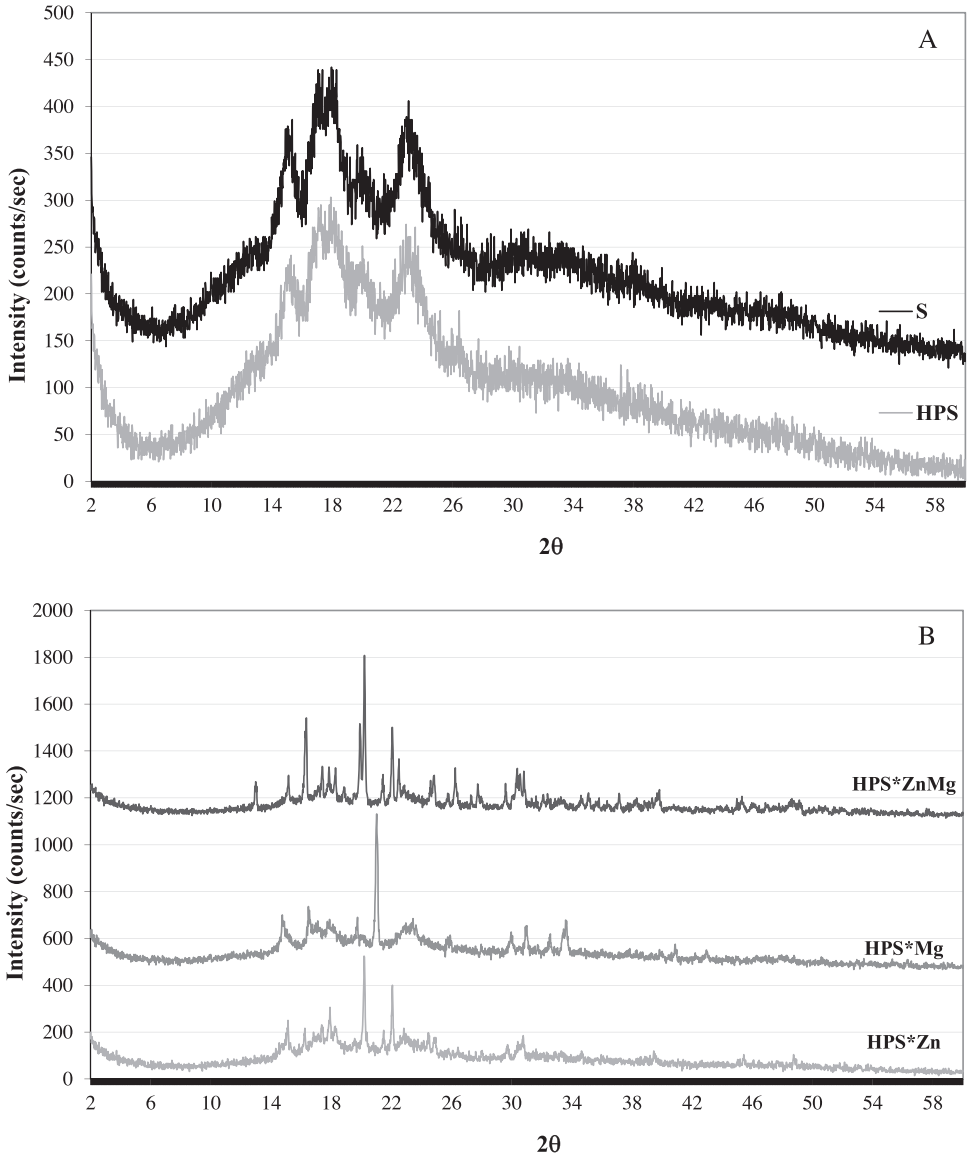

Fig. 5 – X-ray diffraction pattern of (A) Native (S) and HPS carriers, (B) *in situ* high pressure treated bioactive starches. Nomenclature is referred in Table 1.

This fact maybe attributed to a preferential adsorption of mineral salt in *in situ* treated samples as observed in Fig. 4.

The crystalline fraction of starch carriers and bioactive starches is shown in Fig. 6. For carriers without active compound, the crystalline fraction was higher for S than for HHP treated starch, due to a partial gelatinization of the corn starch granules which occurred during the high pressure treatment. However, the presence of mineral salts contributed to the overall crystalline fraction, increasing this parameter in all cases. Among the samples with mineral salts, those generated by *in situ* high pressure treatment showed the highest crystalline fraction (Fig. 6). The CF attributed to the mineral incorporation increased in the following order: S < HPS < HPS*.

3.2.3. *Differential scanning calorimetry*

Starch carriers thermograms showed an endothermic peak at 69.8 °C for native corn starch and 68.6 °C for high pressure treated starch (Table 2). The shift in the peak temperature was attributed to a partial gelatinization during high pressure treatment as this change was also observed in the crystalline fraction determined by X-ray diffraction.

In general, all bioactive carriers exhibited higher onset and peak temperatures than their respective starch controls (S and HPS). This fact was attributed to the presence of Zn^{+2} and Mg^{+2}, more precisely, to the interaction between hydroxyl groups of the glucose units and these cations. It appears that the starch granule was stabilized by the presence of the cations, thus more energy was necessary to reach gelatinization temperatures. It is worth noting that regardless the active compound, peak temperatures increased in the following order S < HPS < HPS* (Table 2). This trend was attributed to the increasing concentration of salts in the HHP treated samples, as discussed above (Fig. 4). The cases of HPS^*_{ZnY} and HPS^*_{ZnMg}, should be highlighted since even higher T_p were observed. These results can be directly related to the high zinc sulphate content detected in *in situ* samples. Besides, the raw salt showed a decomposition peak at 80 and 96.5 °C. Luo et al. (2013) studied the preparation and properties of enzyme-modified cassava starch-zinc complexes and observed by FTIR that hydroxyl groups of the glucose units are involved in hydrogen bonds. They proposed that the reduction of hydrogen bonds suggested that the hydroxyl groups

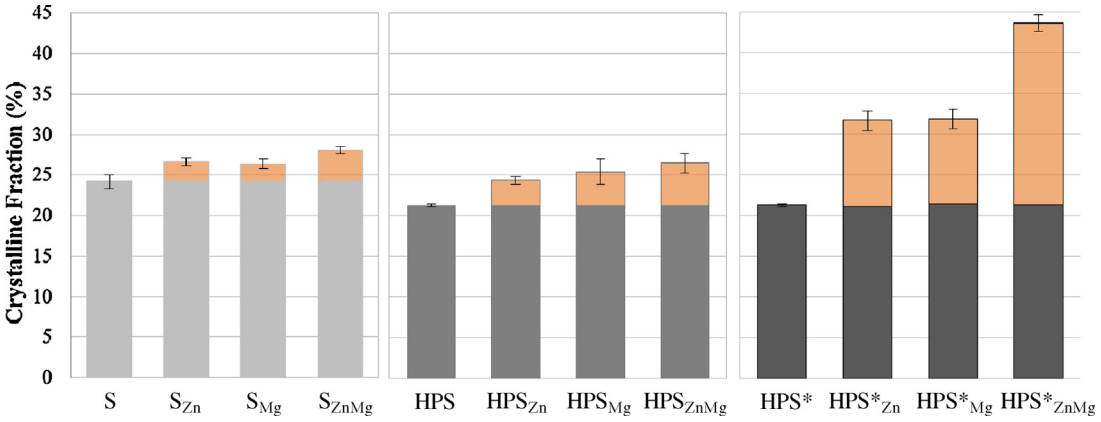

Fig. 6 – Crystalline fraction (%) of starch carriers with and without active compounds. Orange portion in the column represents the mineral crystalline fraction of each sample, while grey portion represents the starch contribution. Nomenclature is referred in Table 1.

might be involved in coordination with zinc. Similar results were found by Staroszczyk and Janas (2010).

Melting enthalpies of native and pressure-treated starches were calculated to analyze the effect of the type of starch and the active compound on the gelatinization degree. The ΔH parameter represents the starch fraction that gelatinizes during DSC experiments; lower enthalpy values would be obtained if the starch granules were previously gelatinized during the HHP treatment. As expected, melting enthalpy decreased from 12.3 J/g for S to 9.9 J/g for HPS (Table 2). Statistical analysis confirmed that active compounds (yerba mate extract and salts) did not affect the melting enthalpy ($p > 0.05$), whereas the type of starch did. Tukey's test showed that the ΔH of samples obtained with both HHP treated starches (*in situ* or immersion) were significantly different from that obtained for samples of S carriers. These results show the extent of the partial gelatinization produced by high pressure treatment under the conditions operated in this work, less energy was necessary to disrupt starch granules when they were previously subjected to HHP.

Table 2 – Thermal parameters obtained from DSC thermograms for control and bioactive starches. Nomenclature is referred to that in Table 1.

Sample	T onset (°C)	T peak (°C)	ΔH (J/g)
S	65.21 ± 1.31	69.89 ± 0.06	12.3 ± 1.60
HPS	65.17 ± 0.41	68.67 ± 0.12	9.92 ± 1.93
S_{Zn}	64.30 ± 0.97	70.19 ± 1.07	10.6 ± 0.03
HPS_{Zn}	66. 97 ± 0.63	71.92 ± 1.02	11.22 ± 0.91
HPS^*_{Zn}	69.20 ± 0.77	73.78 ± 0.35	9.97 ± 1.56
S_{Mg}	65.90 ± 0.15	71.01 ± 0.04	11.05 ± 0.02
HPS_{Mg}	68.32 ± 0.53	72.28 ± 0.20	7.90 ± 1.26
HPS^*_{Mg}	68.81 ± 0.08	74.06 ± 0.47	10.07 ± 2.01
S_{ZnMg}	66.08 ± 0.58	71.49 ± 0.33	9.06 ± 0.92
HPS_{ZnMg}	68.72 ± 0.06	73.33 ± 1.19	8.40 ± 1.54
HPS^*_{ZnMg}	74.92 ± 0.19	80.29 ± 0.01	8.85 ± 0.25
S_{ZnY}	65.43 ± 0.04	70.34 ± 0.21	10.20 ± 0.17
HPS_{ZnY}	67.09 ± 0.30	71.28 ± 0.30	7.29 ± 0.21
HPS^*_{ZnY}	81.52 ± 0.25	87.49 ± 0.52	7.40 ± 1.73
S_{MgY}	66.31 ± 0.05	71.84 ± 0.24	10.41 ± 0.04
HPS_{MgY}	66.88 ± 1.06	71.39 ± 1.17	8.545 ± 1.29
HPS^*_{MgY}	70.52 ± 0.25	74.55 ± 0.03	11.40 ± 1.84
S_{ZnMgY}	65.77 ± 0.66	71.17 ± 0.35	11.54 ± 1.15
HPS_{ZnMgY}	68.29 ± 0.42	72.95 ± 0.79	10.44 ± 2.22
HPS^*_{ZnMgY}	69.81 ± 0.30	74.78 ± 0.13	11.10 ± 1.43

According to Liu et al. (2008), lowered melting energy of the crystalline regions could be due to a partial melting of the crystalline structure during high pressure compression or an alteration of the crystalline structure. In the present work, alteration of the crystalline structure was discarded by X-ray diffraction analyses because a typical "A" pattern was maintained after HHP treatment. Moreover, Łabanowska et al. (2013) reported that the ionic radius size of the cation physically affects the structure of starch, thus leading to a higher degradation temperature. Accordingly, in our results the presence of zinc showed more effect than magnesium.

Jane (1993) also reported an increase in T_p and ΔH for corn starch in the presence of SO_4^{2-} ions, when studying the mechanism of starch gelatinization in neutral salt solutions. According to this author, this behavior was due to the strong interaction of these ions with water molecules and the consequent reduction in the fraction of free water molecules; the solution viscosity also increased retarding the diffusion of ions into the granule. Besides, there would be repulsion between the hydroxyl groups of the starch and the SO_4^{2-} groups, contributing to the resistance of the starch to gelatinization.

3.3. *Loading of active compounds in bioactive starches*

With respect to the mineral content, the starch treatment was a significant factor as detected by atomic emission spectrometry (Fig. 7). An increasing order of mineral loading was observed: S < HPS < HPS*, as was also observed by SEM–EDX (Fig. 4). The combinations of HPS* with Zn had the highest values. Addition of yerba mate extract increased Zn concentration in the *in situ* HHP samples, however a decrease in Mg content was observed for this treatment. The same behavior was observed when the two salts were incorporated together with the yerba mate extract.

Extensive studies of the interaction of metal ions with various types of native and modified starches have shown that ions bind to functional groups of starch in different ways (Ciesielski et al., 2003; Łabanowska et al., 2013; Lai et al., 2001). For the alkali-earth metal ions, it is postulated that they can form complexes with starch, but also as for alkali metal ions, there are electrostatic interactions between the cations and anions interacting with OH groups. The sorption properties

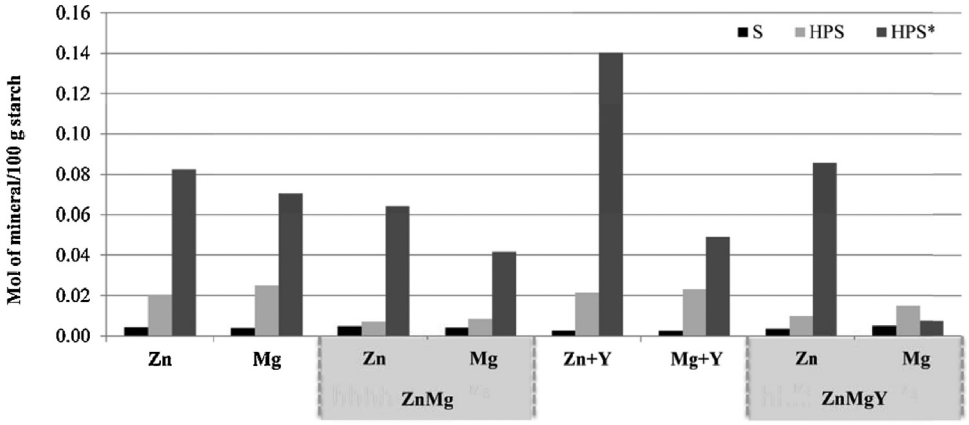

Fig. 7 – Mineral content of bioactive carriers. Maximum standard deviation was 0.0009 for Zn and 0.00004 for Mg. Nomenclature is referred in Table 1.

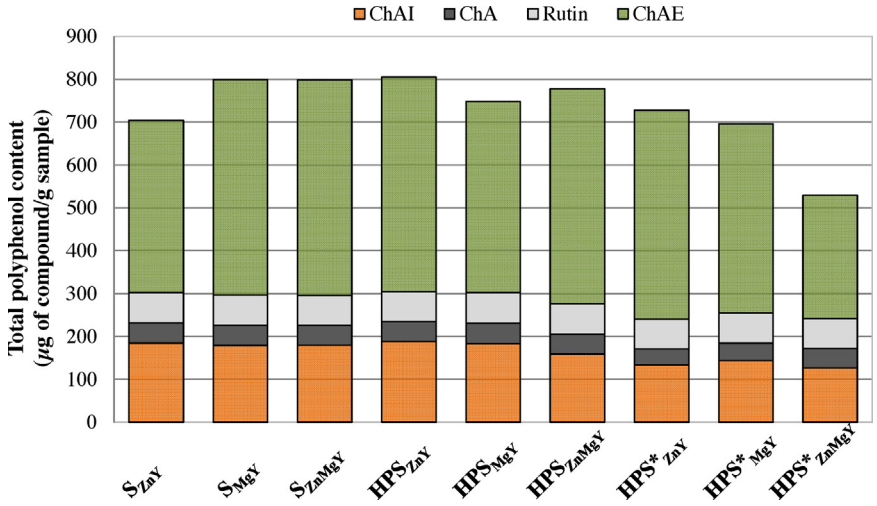

Fig. 8 – Effect of mineral presence and type of starchcarrier on the total polyphenol content of yerba mate determined by HPLC-UV.S = Non treated starch, HPS = HP treated starch obtained by immersion and HPS* = HP treated starch obtained *in situ*. Nomenclature of samples is referred in Table 1. CHAI = Chlorogenic acid isomers, CHA = Chlorogenic acid and CHAE = Chlorogenic acid esters.

of starch in the interaction with these metal ions cannot be excluded, as well.

With respect to the polyphenol content detected by the Folin–Ciocalteau method, the total amount of polyphenols in control samples (starches loaded with only yerba mate) was 1 mg compounds/g starch. Similar values were found for all samples after the HHP treatment, except for those containing zinc, which showed lower values of polyphenol content (0.88 mg/g starch).

Fig. 8 shows the total polyphenol content determined by HPLC in bioactive starches. When analyzing polyphenol composition, all samples had the same relative amounts of the different polyphenols chlorogenic acid esters (55%): chlorogenic acid isomers (27%): chlorogenic acid (8%): rutin (10%). The same relationship was found for yerba mate lyophilized extracts (Deladino et al., 2014).

The starch treatment did not affect polyphenol loading for S and HPS samples. However, lower values were found for HPS* one (Fig. 8). This behavior could be attributed to the higher amount of minerals loaded in HPS* starches, as can be seen in Fig. 7, which caused a decrease in polyphenols loading. Moreover, this effect was more marked in HPS^*_{ZnMgY} samples when both zinc and magnesium were combined with yerba mate extract under pressure. In a previous work (Deladino et al., 2014) HPS* samples gave the highest values of polyphenol content when the starches were loaded with only yerba mate extract. These results confirm the hypothesis that minerals, instead of yerba mate, would occupy free sites of the starch granule when both of these compounds simultaneously undergo the high pressure treatment.

4. Conclusions

Corn starch was suitable to carry mineral salts and yerba mate extract simultaneously. High hydrostatic pressure treatment improved the starch's ability to carry bioactive compounds, for both, minerals and yerba mate polyphenols. This advantage was related to an increase in the quantity of pores of partially gelatinized starch. Besides, in general, the loading of minerals was favored when active compounds were incorporated by the *in situ* HHP treatment. At the same time, native starch was also able to transport both vehicle minerals and yerba mate extract, although in lesser quantities.

Zinc sulphate showed a preferential absorption in comparison with magnesium; however, it adversely affected the polyphenol content in most of the samples with yerba mate. On the other hand, magnesium did not influence polyphenol content.

The presented approach suggests a new strategy of combining multiple ingredients in a simple carrier such as corn starch. These bioactive carriers will be suitable additives or ingredients for a wide range of functional foods, such as soups, bakery products, desserts and other powder formulations.

Acknowledgements

Work was carried out thanks to the project "CRYODYMINT" (AGL2010-21989-C02-02) Spanish Science and Innovation Ministry, and the financial support of PRASY, Instituto Nacional de la Yerba Mate (INYM), Argentina. A.S. Teixeira was supported by CSIC, *via* the JAE-Pre program, partially funded from ESF. Dr. Pedro D. Sanz from ICTAN, Grupo de Procesos Innovadores y Calidad en Alimentos (INNOTECHFOOD), CSIC, Spain, is gratefully acknowledged for providing the use of the optical microscope. Dr. Miguel A. Peña, Research Scientist, Institute of Catalysis and Petrochemistry, CSIC, Madrid, for his help in the interpretation of X-Ray diffraction patterns. The authors would like to thank Christopher Young, P.E. for his help with the English language In memory of Dr. Miriam Martino (1958-2014). Lead Scientist, CIDCA-CONICET, Argentina. A highly respected colleague, mentor and friend of many years, who will be greatly missed.

References

Anderson, R., Conway, H., Pfeifer, V., Griffin, E., 1969. Gelatinization of corn grits by roll and extrusion cooking. Cereal Sci. Today, 14.

Aparicio, C., Resa, P., Elvira, L., Molina-García, A.D., Martino, M., Sanz, P.D., 2009. Assessment of starch gelatinization by ultrasonic and calorimetric techniques. J. Food Eng. 94, 295–299.

Beirão-da-Costa, S., Duarte, C., Moldão-Martins, M., Beirão-da-Costa, M.L., 2011. Physical characterization of rice starch spherical aggregates produced by spray-drying. J. Food Eng. 104, 36–42.

Bouis, H.E., Chassy, B.M., Ochanda, J.O., 2003. 2. Genetically modified food crops and their contribution to human nutrition and food quality. Trends Food Sci. Technol. 14, 191–209.

Bracesco, N., Sanchez, A.G., Contreras, V., Menini, T., Gugliucci, A., 2011. Recent advances on *Ilex paraguariensis* research: minireview. J. Ethnopharmacol. 136, 378–384.

Carvalho, A.J.F., 2013. 7—Starch: Major Sources, Properties and Applications as Thermoplastic Materials, Handbook of Biopolymers and Biodegradable Plastics. William Andrew Publishing, Boston, pp. 129–152.

Ciesielski, W., Lii, C.-y., Yen, M.-T., Tomasik, P., 2003. Interactions of starch with salts of metals from the transition groups. Carbohydr. Polym. 51, 47–56.

Chiang, B.Y., Johnson, J.A., 1977. Measurement of total and gelatinized starch by glucoamylase and o-toluidine reagent. Cereal Chem. 54, 429–435.

Deladino, L., Anbinder, P.S., Navarro, A.S., Martino, M.N., 2008. Encapsulation of natural antioxidants extracted from *Ilex paraguariensis*. Carbohydr. Polym. 71, 126–134.

Deladino, L., Teixeira, A.S., Navarro, A.S., Alvarez, I., Molina-García, A.D., Martino, M., 2014. Corn starch systems as carriers for yerba mate (*Ilex paraguariensis*) antioxidants. Food Bioprod. Process., ⟨http://dx.doi.org/10.1016/j.fbp.2014.07.001⟩.

Douzals, J.P., Cornet, J.M.P., Gervais, P., Coquille, J.C., 1996. Hydration and pressure–temperature phase diagram of wheat starch. J. Agric. Food Chem. 44, 1403–1408.

Etcheverry, P., Grusak, M.A., Fleige, L.E., 2012. Application of in vitro bioaccessibility and bioavailability methods for calcium, carotenoids, folate, iron, magnesium, polyphenols, zinc and vitamins B6, B12, D, and E. Front. Physiol. 3 (317), 1–22.

Fernández, P.P., Sanz, P.D., Martino, M.N., Molina-García, A.D., 2008. Partially-gelatinised starches by high hydrostatic pressure as oligoelement carriers. Span. J. Agric. Res. 6, 129–137.

Filip, R., Sebastian, T., Ferraro, G., Anesini, C., 2007. Effect of Ilex extracts and isolated compounds on peroxidase secretion of rat submandibulary glands. Food Chem. Toxicol. 45, 649–655.

Fornal, J., Sadowska, J., Błaszczak, W., Jeliński, T., Stasiak, M., Molenda, M., Hajnos, M., 2012. Influence of some chemical modifications on the characteristics of potato starch powders. J. Food Eng. 108, 515–522.

Fu, Z.-q., Wang, L.-j., Zou, H., Li, D., Adhikari, B., 2014. Studies on the starch–water interactions between partially gelatinized corn starch and water during gelatinization. Carbohydr. Polym. 101, 727–732.

Genc, Y., Humphries, J., Lyons, G., Graham, R., 2005. Exploiting genotypic variation in plant nutrient accumulation to alleviate micronutrient deficiency in populations. J. Trace Elem. Med. Biol. 18, 319–324.

Gorzalczany, S., Filip, R., Alonso, M.a.d.R., Miño, J., Ferraro, G.E., Acevedo, C., 2001. Choleretic effect and intestinal propulsion of 'mate' (*Ilex paraguariensis*) and its substitutes or adulterants. J. Ethnopharmacol. 75, 291–294.

Graham, R.D., Welch, R.M., Bouis, H.E., 2001. Addressing Micronutrient Malnutrition through Enhancing the Nutritional Quality of Staple Foods: Principles, Perspectives and Knowledge Gaps, Advances in Agronomy. Academic Press, pp. 77–142.

Grusak, M.A., Cakmak, I., 2005. Methods to improve the crop-delivery of minerals to humans and livestock. In: Broadley, M.R., White, P.J. (Eds.), Plant Nutritional Genomics. Blackwell Publishing, Oxford, pp. 265–286.

Hamdaoui, M., Hédhili, A., Doghri, T., Tritar, B., 1997. Effect of tea decoction given to rats ad libitum for a relatively long time on body weight gains and iron, copper, zinc, magnesium concentrations in blood, liver, duodenum and spleen. Ann. Nutr. Metab. 41, 196–202.

Heck, C.I., González de Mejía, E., 2007. Yerba mate tea (*Ilex paraguariensis*): a comprehensive review on chemistry, health implications, and technological considerations. J. Food Sci. 72, R138–R151.

Jane, J.-L., 1993. Mechanism of starch gelatinization in neutral salt solutions. Starch 45, 161–166.

JCPDS, 1999. Database for Standard Reference Materials from Joint Committee on Powder Diffraction Standards (JCPDS), USA.

Katopo, H., Song, Y., Jane, J.-l., 2002. Effect and mechanism of ultrahigh hydrostatic pressure on the structure and properties of starches. Carbohydr. Polym. 47, 233–244.

Łabanowska, M., Kurdziel, M., Bidzińska, E., Fortuna, T., Pietrzyk, S., Przetaczek-Roznowska, I., Roznowski, J., 2013. Influence of metal ions on thermal generation of carbohydrate radicals in native and modified starch studied by EPR. Starch 65, 469–482.

Lai, V.M.F., Tomasik, P., Yen, M.-T., Hung, W.-L., Lii, C.-y., 2001. Re-examination of the interactions between starch and salts of metals from the non-transition groups. Int. J. Food Sci. Technol. 36, 321–330.

Le Corre, D.b., Bras, J., Dufresne, A., 2010. Starch nanoparticles: a review. Biomacromolecules 11, 1139–1153.

Liu, Y., Selomulyo, V.O., Zhou, W., 2008. Effect of high pressure on some physicochemical properties of several native starches. J. Food Eng. 88, 126–136.

López, O.V., García, M.A., 2012. Starch films from a novel (*Pachyrhizus ahipa*) and conventional sources: development and characterization. Mater. Sci. Eng., C 32, 1931–1940.

Luo, Z., Cheng, W., Chen, H., Fu, X., Peng, X., Luo, F., Nie, L., 2013. Preparation and properties of enzyme-modified cassava starch–zinc complexes. J. Agric. Food Chem. 61, 4631–4638.

Mali, S., Grossmann, M.V.E., García, M.A., Martino, M.N., Zaritzky, N.E., 2006. Effects of controlled storage on thermal, mechanical and barrier properties of plasticized films from different starch sources. J. Food Eng. 75, 453–460.

Meenakshi, J.V., 2009. Biofortification. Best Practice Paper: New Advice from CC08. Copenhagen Consensus Center, Denmark.
Paulik, J., Paulik, F., Arnold, M., 1981. Dehydration of magnesium sulphate heptahydrate investigated by quasi isothermal-quasi isobaric TG. Thermochim. Acta 50, 105–110.
Pfeiffer, W.H., McClafferty, B., 2007. HarvestPlus: breeding crops for better nutrition. Crop Sci. 47, 88–105.
Poletti, S., Gruissem, W., Sautter, C., 2004. The nutritional fortification of cereals. Curr. Opin. Biotechnol. 15, 162–165.
Rodrigues, A., Emeje, M., 2012. Recent applications of starch derivatives in nanodrug delivery. Carbohydr. Polym. 87, 987–994.
Rude, R.K., Gruber, H.E., 2004. Magnesium deficiency and osteoporosis: animal and human observations. J. Nutr. Biochem. 15, 710–716.
Simonin, H., Guyon, C., Orlowska, M., de Lamballerie, M., Le-Bail, A., 2011. Gelatinization of waxy starches under high pressure as influenced by pH and osmolarity: gelatinization kinetics, final structure and pasting properties. LWT Food Sci. Technol. 44, 779–786.
Spiess, M., Gruehn, R., 1979. Beiträge zum thermischen Verhalten von Sulfaten. II. Zur thermischen Dehydratisierung des $ZnSO_4 \cdot 7H_2O$ und zum Hochtemperaturverhalten von wasserfreiem $ZnSO_4^+$. Z. Anorg. Allg. Chem. 456, 222–240.
Staroszczyk, H., Janas, P., 2010. Microwave-assisted synthesis of zinc derivatives of potato starch. Carbohydr. Polym. 80, 962–969.
Stolt, M., Stoforos, N.G., Taoukis, P.S., Autio, K., 1999. Evaluation and modelling of rheological properties of high pressure treated waxy maize starch dispersions. J. Food Eng. 40, 293–298.
Stute, R., Klingler, R.W., Boguslawski, S., Eshtiaghi, M.N., Knorr, D., 1996. Effects of high pressures treatment on starches. Starch 48, 399–408.
Tao, Y., Sun, D.-W., Górecki, A., Blaszczak, W., Lamparski, G., Amarowicz, R., Fornal, J., Jeliński, T., 2012. Effects of high hydrostatic pressure processing on the physicochemical and sensorial properties of a red wine. Innovative Food Sci. Emerg. Technol. 16, 409–416.
Thacher, T., Fischer, P., Strand, M., Pettifor, J., 2006. Nutritional rickets around the world: causes and future directions. Ann. Trop. Paediatr. 26, 1–16.
Walenta, K., 1978. Boyleite, a new sulfate mineral from Kropbach, southern Black Forest. Chem. Erde 37, 73–79.
White, P.J., Broadley, M.R., 2005. Biofortifying crops with essential mineral elements. Trends Plant Sci. 10, 586–593.
Wootton, M., Weedon, D., Munk, N., 1971. A rapid method for the estimation of starch gelatinization in processed foods. Food Technol. Austr. 23, 612–615.